OPEN ACCESS

Effect of stretching on the molecular conformation of oligo (ethylene oxide): a theoretical study

New Journal of Physics
An Institute of Physics and Deutsche Physikalische Gesellschaft Journal

Effect of stretching on the molecular conformation of oligo (ethylene oxide): a theoretical study

H J Kreuzer†, R L C Wang† and M Grunze‡

† Department of Physics, Dalhousie University, Halifax, NS, Canada B3H 3J5
‡ Angewandte Physikalische Chemie am Physikalisch-Chemischen, Institut der Universität Heidelberg, Im Neuenheimer Feld 253, D-69120 Heidelberg, Germany
E-mail: kreuzer@is.dal.ca

New Journal of Physics **1** (1999) 21.1–21.16 (http://www.njp.org/)
Received 13 June 1999; online 26 November 1999

Abstract. The force–extension measurements on simple poly(ethylene glycol) molecules by Oesterfelt *et al* in different solvents can be quantitatively explained based on *ab initio* quantum mechanical calculations of the potential energy surfaces of the polymer segments in vacuum and in the solvated form. The proper statistical mechanical calculations of the force–extension relation, both for isothermal–isochoric and isothermal–isobaric conditions (the latter appropriate to the experimental set-up), demonstrate, that in the low-force regime transitions from the amorphous to the helical conformers, and in the high-force regime stretching of the helical to the planar 'all-trans' conformer occur. The presence of water affects all but the 'all-trans' conformer by shortening and stiffening.

Contents

1367-2630/99/000021+16$30.00

1. Introduction

Single-molecule force microscopy has been a versatile and powerful tool to measure binding forces of receptor ligand systems [1, 2], to observe the unfolding of protein domains [3] or to measure the elastic properties of individual macromolecules [4]. In a recent paper Oesterhelt *et al* [6] reported force measurement on individual poly (ethylene glycol) chains (PEG)† which were fixed to a substrate by covalent bonds and elongated using an atomic force microscope (AFM) tip. The measurements showed that the forces necessary to stretch the polymer chains depend strongly on the solvent surrounding the molecule, i.e. PBS buffer or hexadecane. In the low- and high-force regime the measurements show no difference between the polar and non-polar solvents. In the stretched regime, before rupture occurs, the elasticity is dominated by the stiffness of the bond angle potentials, which are expected not to depend on the surrounding solvent. However, in the intermediate-force regime the elongation observed at constant force is substantially smaller in PBS buffer than in hexadecane.

For a discussion of these results we have to recall the possible molecular conformations of the ethylene oxide (EG) units in PEG. The helical structure of PEG is characteristic for the crystalline state of the polymer, and it is locally retained when the polymer is dissolved in water. In the helical structure of PEG the bonds of the backbone are arranged in a trans–gauche–trans (tgt) order, where the gauche angle is rotated uniformly with respect to the –C–C–O plane over the length of the helix, either clockwise or counterclockwise ($(+)$ or $(-)$). Introduction of gauche rotations other than those characteristic for the uniform helix leads to a gauche defect and ultimately to an amorphous conformation in which the sense of gauche rotation between the ethylene oxide units is arbitrary. Accordingly, the overall length of the polymer chain depends on the concentration of gauche defects. In the stretched planar 'all-trans' form (ttt), which can be obtained by mechanically stretching the polymer, the chain is fully extended. Hence, with increasing contour length of the polymer chain, the conformation will change from an amorphous via a helical to a planar 'all-trans' structure. All these conformations are likely to occur with contour-length-dependent statistical weight in the force versus extension measurements of Oesterhelt *et al* [6], since the polymer used had a molecular weight distribution of around 30 000 Daltons, which corresponds to about 750 ethylene oxide units.

Oesterhelt *et al* [6] propose that the stabilization in PBS buffer arises from the solvation of the polymer, and discuss a model for the interaction of water with the ethylene oxide moieties as proposed previously by us [5]. In our *ab initio* calculations on the interaction of water with the helical and planar 'all-trans' conformers of methoxy-tri(ethylene oxide) undecanethiolate in self-assembled monolayers on gold and silver substrates we found, that two next-nearest oxygen atoms in a tgt–tgt helical conformation generate a strong dipolar field in which a water molecule can bind in two different ways, either via a single hydrogen bridge bond or in a double-bridge mode (see figure 3 [5]). In the stretched ttt conformation the distance between the oxygens is too large so that the water molecules can only interact with a single oxygen. The difference in binding energy of water to the tgt–tgt and ttt–ttt conformers is about $+180$ meV‡. Accordingly, water stabilizes the ttg conformers with respect to the stretched ttt structure and the solvation shell constitutes a barrier towards stretching the polymer chain. Hexadecane does not interact

† PEG is also referred to as poly(ethylene oxide) (PEO) and poly(oxyethylene) (POE). In this paper, we will use the term poly(ethylene glycol) (PEG) for polymers or oligomers of all molecular weights.

‡ 100 meV = 9.65 kJ mol^{-1} = 2.305 kcal mol^{-1}.

strongly with the ethylene oxide moeities and hence does not contribute to the stabilization of a particular conformer.

Oesterhelt *et al* [6] have analysed their data on the basis of the freely jointed chain model of elastically coupled two-level systems which yields a force–extension relation†

$$L(F) = N_{\mathrm{s}}\left[\frac{L_{\mathrm{planar}}}{\mathrm{e}^{\Delta G/k_{\mathrm{B}}T}+1} + \frac{L_{\mathrm{helical}}}{\mathrm{e}^{-\Delta G/k_{\mathrm{B}}T}+1}\right][\coth(FL_{\mathrm{K}}/k_{\mathrm{B}}T) - k_{\mathrm{B}}T/FL_{\mathrm{K}}] + N_{\mathrm{s}}F/K_{\mathrm{s}}. \quad (1)$$

Here

$$\Delta G(F) = G_{\mathrm{planar}} - G_{\mathrm{helical}} - F[L_{\mathrm{planar}} - L_{\mathrm{helical}}] \quad (2)$$

is the difference in Gibbs free energy between a planar and a helical EG subunit in the presence of a force F with L_{planar} and L_{helical} their respective lengths (in the absence of the force). The Kuhn length L_{K} ($= 7$ Å), the stretching modulus (or segment elasticity) K_{S} ($= 150$ N m^{-1}) and L_{helical} ($= 2.8$) are fitted to the experiments with $L_{\mathrm{planar}} = 3.58$ estimated from bond lengths and angles of the planar 'all-trans' (ttt) structure. This results in $\Delta G = (3 \pm 0.3)k_{\mathrm{B}}T$ which is consistent with prior *ab initio* calculations. Note that for these numbers the last term in equation (1) is negligible up to forces in the nanonewton regime, and the entropy contribution, the square bracket involving the Kuhn length, is unity for forces larger than about 10 pN.

As discussed by Oesterhelt *et al* [6], the elastic response of PEG can be grouped into three regimes: initial small forces have to overcome the entropy elasticity (well described by the freely joined chain model) to uncurl the molecule into a straight, unstretched more or less linear chain of random sequences of ttt and tgt EG subunits with the gauche rotation both clockwise (g^+) and anticlockwise (g^-). When forces reach the piconewton level a supramolecular reorganization occurs in that the shorter units, having one or more gauche rotations, are converted into longer 'all-trans' (ttt) units. After this is completed bond-angle deformation in the all-trans conformer sets in when forces reach hundreds of piconewton.

In this paper we will set up the statistical mechanics of the late stages of the elastic response, i.e. in the regimes of supramolecular reorganization and of bond angle deformation. Such a first-principles theory must (i) calculate the energy spectrum (or the density of states) for PEG chains from quantum mechanics, and (ii) derive the proper statistical ensemble appropriate for the given experiment.

In the next section we outline the theoretical framework. Examples of relevant energy surfaces and excitation spectra and the resulting force–extension curves are presented and discussed in section 3.

2. Theory

2.1. Energy spectrum

Our first task is to calculate the energy spectrum of oligo(ethylene oxide) as a function of chain length for a given number of EG units. Most recent studies of hydrogen-bonded systems use the monoreference formulation of the MP2 method to obtain precise results including correlation effects. As in our previous work [5] we will use the GAUSSIAN 94 suite of programs at the MP2/6-31++G**//HF/3-21G level. As such calculations grow in hardware requirements (memory and CPU time) at least with the fourth (HF) and sixth (MP2) power of the size of the

† Here we have corrected a misprint of the sign in front of ΔG in the exponentials of equation (2) in [6].

Table 1. Energies E_{B}, relative to the energy of the helical conformer ($100\ \mathrm{meV} = 9.65\ \mathrm{kJ\ mol^{-1}} = 2.305\ \mathrm{kcal\ mol^{-1}}$), dihedral angles and molecular lengths, L, between the outermost O atoms (with the distance between outermost C atoms in brackets) of various conformers of $\mathrm{CH_3(EG)_3OCH_3}$.

	Conformation	Dihedral angles	$L(\mathrm{O_1}$–$\mathrm{O_4})$ (Å)	E_{B} (meV)
1	$g^+g^+(0)$	71.9; 73.2; 0.0	7.26(9.03)	394.14
2	$g^+g^+g^+$	71.7; 71.6; 71.7	8.27(10.01)	0.0
3	$g^+g^+(120)$	71.7; 71.2; 120.0	8.71(10.43)	104.49
4	g^+g^+t	71.7; 71.2; 179.7	8.52(10.09)	0.52
5	$g^+g^+(240)$	72.0; 71.3; 240.0	7.67(9.09)	114.04
6	$g^+g^+g^-$	72.2; 72.6; 287.8	6.97(8.41)	26.29
7	ttg^+	180.2; 179.5; 71.3	9.56(11.96)	6.69
8	ttt	180.0; 180.0; 180.0	10.56(12.91)	19.21

basis set (number of electrons) we restrict ourselves in this first paper on the subject to a rather small, but, as we will see, large enough molecule, namely $\mathrm{CH_3(EG)_nOCH_3}$ with $n = 3$, where EG is our abbreviation for $\mathrm{OCH_2CH_2}$.

We have done MP2 calculations and find that for $(\mathrm{EG})_3$ the helical conformer is the most stable. Energies (relative to the energy of the stablest helical conformer), molecular lengths and dihedral angles of various conformers and the energy barriers between the local minima are listed in table 1. The molecular length is the distance between the outermost oxygen atoms so that a third of it can be interpreted as the (average) length of one EG subunit; we also list the distance between the outermost carbons in brackets. In all the conformations listed we keep all the C–O bonds in the trans configuration and omit this information from our notation, i.e. the helical conformer $(tg^+t$–tg^+t–$tg^+t)$ is denoted as $(g^+g^+g^+)$. The conformations 1, 3 and 5 are activation barriers along the dihedral counterclockwise rotation between the adjacent conformers.

Solid-sphere models of the four most relevant conformers, $(g^+g^+g^-)$, $(g^+g^+g^+)$, (g^+tt) and (ttt), are shown in figure 1. It is important to note how close in energy the various conformers are and how small the barriers are between these local minima. We should add as a cautionary note that Hartree–Fock calculations without the MP2 corrections yield a different (i.e. wrong) sequence of stability, making for instance the 'all-trans' conformer more stable than the helical one, and also increasing the barriers considerably.

To find the part of the energy spectrum of an $(\mathrm{EG})_3$ molecule relevant to understanding the force–extension relation, we calculate the ground state energy and vibrational excitations of the energetically lowest conformers as a function of their length over such a range that the different energy curves overlap sufficiently. As the length of a given conformer changes, its internal structure, i.e. bond lengths and angles, are allowed to adjust self-consistently. As the length of a given conformer is changed sufficiently so that it is close to the length of another conformer at its lowest energy, the conformational structure of the former can no longer be kept in the self-consistent calculations and there is a spontaneous transformation to the latter. As an example the helical $(g^+g^+g^+)$ conformer changes spontaneously at $L \simeq 9$ into the (g^+tt) structure. In a given *ab initio* calculation we impose the boundary conditions such that the distance between the first and last carbon atom in the chain is held fixed. This length L

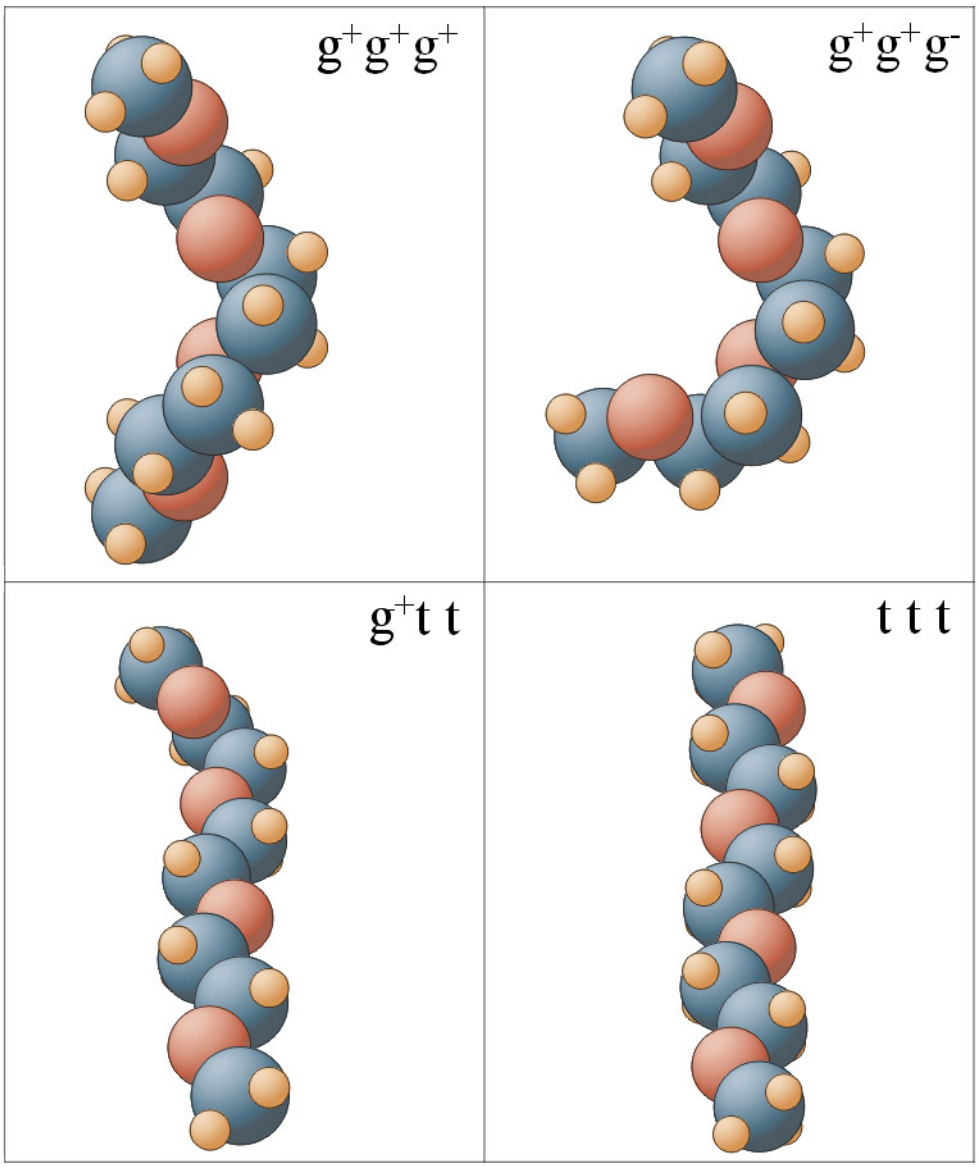

Figure 1. Solid sphere models of the $(g^+g^+g^-)$, $(g^+g^+g^+)$, (g^+tt) and (ttt) conformers of $(\mathrm{EG})_3$.

will be varied from slightly below the length of the $g^+g^+g^-$ (amorphous) conformer and a value beyond the length of the 'all-trans' conformer. Because various conformers of $(\mathrm{EG})_n$, for a given length, can be within less than 100 meV in energy we will calculate the energy, $V_i(L)$, for a few of the lowest such states that are likely to contribute to the elastic response at room temperature. We will also calculate the normal mode frequencies, $\nu_k^{(i)}(L)$, for each conformer.

The ground state energy curves for the $(g^+g^+g^-)$, $(g^+g^+g^+)$, (g^+tt) and (ttt) conformers are shown in figure 2. We have not included the (g^+g^+t) conformer because its potential minimum

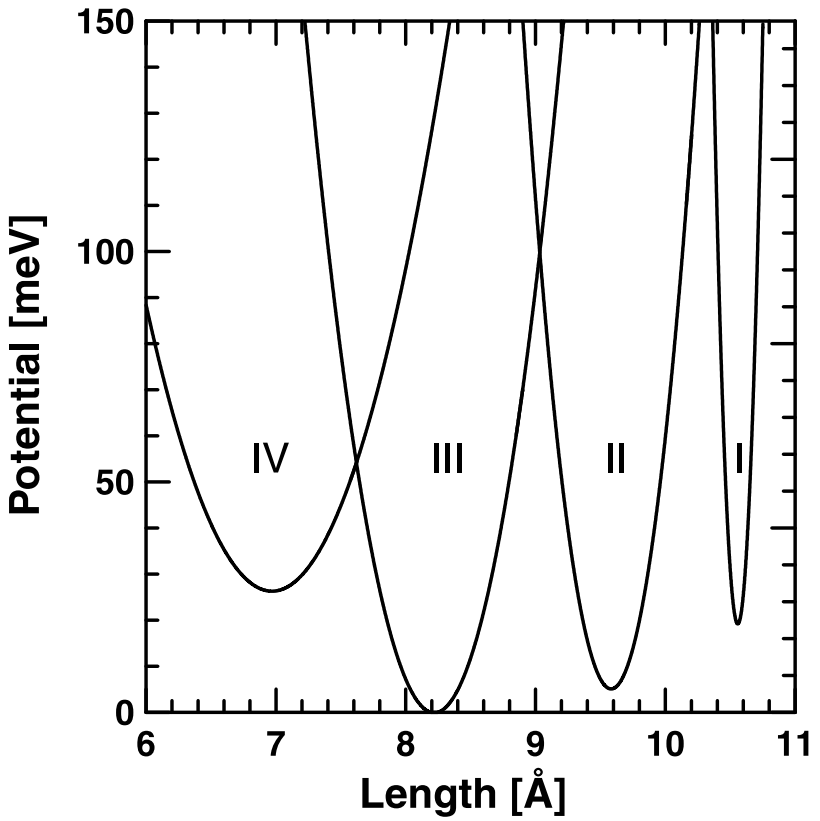

Figure 2. Ground state energy curves for the $(g^+g^+g^-)$ (IV), $(g^+g^+g^+)$ (III), (g^+tt) (II) and (ttt) (I) conformers of $(\mathrm{EG})_3$ in vacuum.

is too close to that of $(g^+g^+g^+)$ to make a noticeable contribution to the force–extension curves. We have also calculated the frequencies of the 84 normal modes and the infrared spectra for each conformer, obtaining reasonable agreement with experiment where data are available.

Although the energy curves are not symmetric around their minima, we fit an approximate quadratic dependence on L to extract some average force constants for the four conformers, getting 2.1, 5, 7.5 and 110 N m^{-1} for the $(g^+g^+g^-)$, $(g^+g^+g^+)$, (g^+tt) and (ttt) conformers, respectively. Not surprisingly, the planar conformer is considerably stiffer than the conformers with at least one gauche conformation.

Because we will also look at the influence of water adsorbed on $(\mathrm{EG})_3$ we have calculated the potential energy curves for the four conformers in the presence of water. In a first calculation we added only two water molecules along the strand of each conformer to complete the first hydration shell, in agreement with experimental data that suggest that there is one water molecule strongly bound per EG unit [7]. The addition of two water molecules hardly affects the 'all-trans' conformer, neither in length nor in the shape of its potential energy curve. This is in stark contrast to the other three conformers which, because of the presence of gauche conformations, can bind one or two water molecules by establishing hydrogen bridges to two oxygen atoms along the molecule. This not only leads to significant energy gains relative to the 'all-trans' conformer (typically of the order of 300 meV), but it also shortens these conformers by typically 0.5 Å (or 5–10%), e.g. for the $g^+g^+g^+$ conformer from 8.27 to 7.68 Å. This double hydrogen

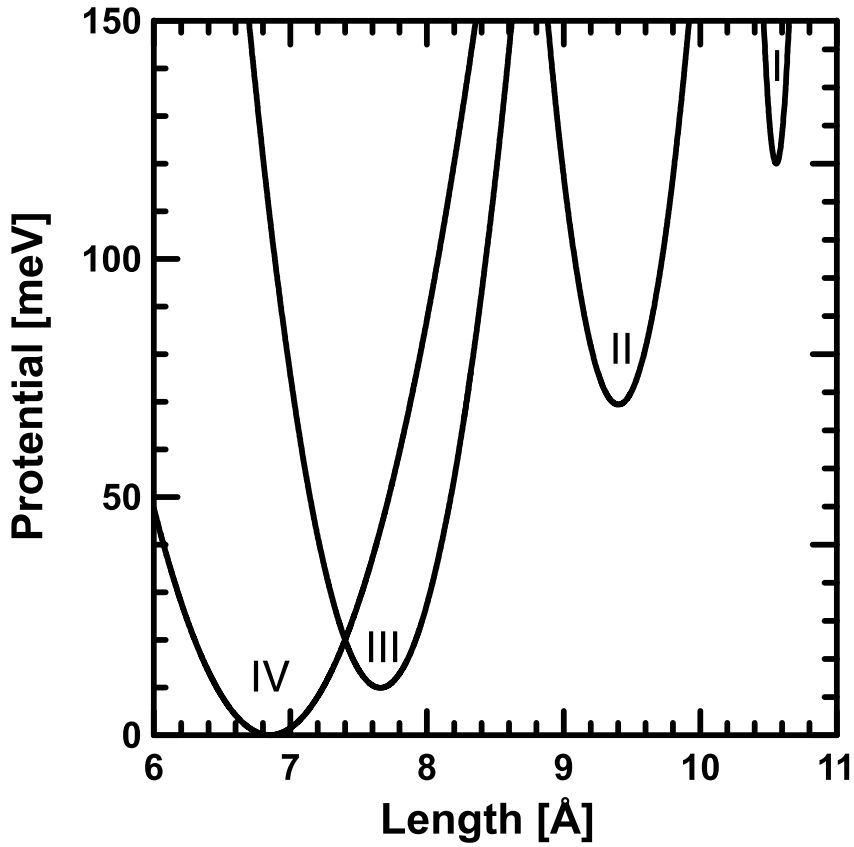

Figure 3. Ground state energy curves for the $(g^+g^+g^-)$ (IV), $(g^+g^+g^+)$ (III), (g^+tt) (II) and (ttt) (I) conformers of solvated $(\mathrm{EG})_3$.

Table 2. Energies, relative to the energy of the helical conformer (100 meV = 9.65 kJ mol^{-1} = 2.305 kcal mol^{-1}), dihedral angles and molecular lengths of the solvated conformers of $\mathrm{CH_3(EG)_3OCH_3}$.

	Conformation	Dihedral angles	$L(\mathrm{O_1}$–$\mathrm{O_4})$ (Å)	E_B (meV)
1	$g^+g^+g^+$	63.7; 62.4; 66.2	7.68	0.0
5	g^+tt		9.38	60
7	$g^+g^+g^-$		6.85	–10
9	ttt	180.0; 180.0; 180.0	10.55	110

bonding is particularly efficient for the $g^+g^+g^-$ conformer. However, the restriction to two water molecules overestimates the effect of solvation because of the neglect of bridge bonding to the second hydration shell. We have therefore also performed calculations with eight water molecules at the Hartree–Fock level and estimated the bond lengths and relative energies of the conformers based on a comparison between the Hartree–Fock and MP2 results of the calculation with two waters. The results are listed in table 2 and the potential energy curves are given in figure 3. Note that all but the 'all-trans' conformer are shortened considerably but that the widths of the curves are only marginally reduced because the stiffening due to the

two to three water molecules in the first hydration shell is largely compensated by the second shell.

A full account of our calculations of the interaction of $(\mathrm{EG})_3$ with water will be given elsewhere when we discuss the conformational changes occurring in the tri(ethylene oxide)-terminated alkanethiolate self-assembled monolayers exposed to water [8].

2.2. Statistical mechanics

The force–extension relation can be measured under different boundary conditions: (i) one can fix the length of the chain molecule and measure the force necessary to maintain this length; this suggests doing the statistical mechanics in the isothermal–isochoric or Helmholtz ensemble. (ii) One can apply a given force and measure the resultant extension of the molecule [9]. The second boundary condition is maintained in the AFM experiment. This suggests doing the statistical mechanics in the isothermal–isobaric or Gibbs ensemble†.

Beginning with the isothermal–isochoric ensemble (fixed length) we get the Helmholtz free-energy molecule in the ensemble as

$$\begin{aligned} f(T,L) &= -k_{\mathrm{B}}T\ln\sum_i Z_i \\ &= -k_{\mathrm{B}}T\ln\Big\{\sum_i \exp[-\beta V_i(L)]\prod_k z_k^{(i)}(L)\Big\} \end{aligned} \tag{3}$$

where $\beta = 1/k_{\mathrm{B}}T$, i labels the different conformers and $z_k^{(i)}(L)$ is the partition function for the kth vibrational/rotational (intramolecular) mode of the ith conformer at length L. the frequencies of these modes are in the range from 1000 to 3000 cm^{-1} so that they are barely excited at room temperature and a harmonic approximation to account for their zero-point motion is acceptable, namely

$$z_k^{(i)}(L) = \frac{\exp[\beta \mathrm{h}\nu_k^{(i)}(L)/2]}{\exp[\beta \mathrm{h}\nu_k^{(i)}(L)] - 1}. \tag{4}$$

We then obtain the average force (taking the z-direction along L)

$$\begin{aligned} \langle F_z(L)\rangle &= -\frac{\partial f(T,L)}{\partial L}\Big|_T \\ &= \Big(\sum_{i'} Z_{i'}\Big)^{-1}\sum_i Z_i\Big(-\frac{\partial V_i}{\partial L} + k_{\mathrm{B}}T\sum_k \frac{\partial}{\partial L}\ln(z_k^{(i)})\Big) \\ &= \Big(\sum_{i'} Z_{i'}\Big)^{-1}\sum_i Z_i\Big(-\frac{\partial V_i}{\partial L} - \frac{1}{2}\sum_k \coth(\beta \mathrm{h}\nu_k^{(i)}/2)\frac{\partial(\mathrm{h}\nu_k^{(i)})}{\partial L}\Big) \\ &\simeq -\Big(\sum_{i'} Z_{i'}\Big)^{-1}\sum_i Z_i \frac{\partial}{\partial L}\Big(V_i + \frac{1}{2}\sum_k \mathrm{h}\nu_k^{(i)}\Big) \end{aligned} \tag{5}$$

where the last line is valid when $\mathrm{h}\nu_k^{(i)} \gg k_{\mathrm{B}}T$ as for the present system. It turns out that the sum over all frequencies does not change very much, i.e. by less than 1%, from one conformer to the other or for different lengths, so that their derivatives contribute negligibly to the average

† In the case of a one-dimensional chain isochoric and isobaric imply constant or fixed length and force, respectively.

force. Neglecting the internal modes and all conformers but the lowest energy one, we recover the simple result $F_z(L) = -\partial\langle V_i\rangle/\partial L$.

In the isothermal–isobaric or Gibbs ensemble (fixed force) we bring the molecules in contact not only with a thermal reservoir at constant temperature but also with a volume reservoir at constant pressure. For our one-dimensional situation the volume reduces to a length and the pressure to a force. The Gibbs free energy per molecule is then given by

$$\exp[-\beta g(T,F_z)] = \sum_i \exp[-\beta g_i(T,F_z)] = \sum_i \sum_L \exp[-\beta[V_i(L) + F_z L]] \prod_k z_k^{(i)}(L). \tag{6}$$

From this we find the average length of a molecule as a function of the applied force as

$$\begin{aligned}\langle L(F_z)\rangle &= \left.\frac{\partial g(T,F_z)}{\partial F_z}\right|_T \\ &= \frac{\sum_i \int_0^\infty l\,\mathrm{d}l \exp[-\beta[V_i(l) + F_z l]] \prod_k z_k^{(i)}(l)}{\sum_i \int_0^\infty \mathrm{d}l \exp[-\beta[V_i(l) + F_z l]] \prod_k z_k^{(i)}(l)} \\ &\simeq \frac{\sum_i \int_0^\infty l\,\mathrm{d}l \exp[-\beta[V_i(l) + F_z l + \frac{1}{2}\sum_k \mathrm{h}\nu_k^{(i)}(l)]]}{\sum_i \int_0^\infty \mathrm{d}l \exp[-\beta[V_i(l) + F_z l + \frac{1}{2}\sum_k \mathrm{h}\nu_k^{(i)}(l)]]}\end{aligned} \tag{7}$$

where the last line is, again, valid when $\mathrm{h}\nu_k^{(i)} \gg k_\mathrm{B}T$ as for the present system. We have also, for numerical expedience, changed the discrete summation over the volumina (lengths) into an integration.

To make the connection with the model used by Oesterhelt *et al* [6] we keep only two energy surfaces, namely those for the 'all-trans' planar and for the helical conformations. In the integrals in the numerator of (7) we then write $l = l - L_i + L_i$ and find after re-arranging terms

$$\begin{aligned}\langle L(F_z)\rangle = &\frac{1}{\exp[\beta\Delta g(F_z)] + 1}[L_\mathrm{p} + I_\mathrm{p}(F_z)\exp[-\beta(F_z L_\mathrm{p} - g_\mathrm{p}(F_z))]] \\ &+ \frac{1}{\exp[-\beta\Delta g(F_z)] + 1}[L_\mathrm{h} + I_\mathrm{h}(F_z)\exp[-\beta(F_z L_\mathrm{h} - g_\mathrm{h}(F_z))]]\end{aligned} \tag{8}$$

where, for $i = \mathrm{h}, \mathrm{p}$,

$$I_i(F_z) = L_0^{-1}\int_0^\infty (l - L_i)\,\mathrm{d}l \exp[-\beta[V_i(l) + F_z(l - L_i)]] \prod_k z_k^{(i)} \tag{9}$$

where L_0 is an arbitrary length scale to convert the ensemble summation over L in (6) into an integral; L_0 will drop out of the calculation at the end. We have also introduced

$$\Delta g(F_z) = g_\mathrm{p}(F_z) - g_\mathrm{h}(F_z) \tag{10}$$

as the difference in the Gibbs free energies per molecule between the planar and helical states, also defined in (2).

Around the equilibrium length of the conformers we can approximate the energy surfaces by harmonic oscillators, i.e. we can write for $i = \mathrm{p}, \mathrm{h}$

$$V_i(l) = E_i + (k_i/2)(l - l_i)^2. \tag{11}$$

If, in addition, we neglect the contributions from the internal modes of the molecules, we can evaluate the Gibbs free energies and the integrals in equation (8) to get

$$\exp[-\beta g_i(T,F_z)] = L_0^{-1}\sqrt{\frac{\pi k_\mathrm{B}T}{4k_i}}\exp[-\beta(E_i + F_z l_i - F_z^2/4k_i)] \times\Big[1+\mathrm{erf}\Big[\sqrt{\beta k_i}\,|-l_i + F_z/2k_i|\,\Big]\Big] \tag{12}$$

$$I_i(T,F_z) = (l_i - F_z/2k_i)\exp[-\beta g_i(T,F_z)] + \frac{k_\mathrm{B}T}{2k_i}\exp[-\beta(E_i + k_i l_i^2)]. \tag{13}$$

Here $\mathrm{erf}(x)$ is the error function. Inserted in (8) we get

$$\langle L(F_z)\rangle = \frac{L_\mathrm{p} - F_z/2k_\mathrm{p}}{\exp[\beta\Delta g(F_z)]+1}\left[1 - \frac{1}{L_o}\sqrt{\frac{k_\mathrm{B}T}{k_P}}\exp[-\beta(E_\mathrm{p} + k_\mathrm{p}L_\mathrm{p}^2 - g_\mathrm{p}(F_z))]\right] + \frac{L_\mathrm{h} - F_z/2k_\mathrm{h}}{\exp[-\beta\Delta g(F_z)]+1}\left[1 - \frac{1}{L_o}\sqrt{\frac{k_\mathrm{B}T}{k_\mathrm{h}}}\exp[-\beta(E_\mathrm{h} + k_\mathrm{h}L_\mathrm{h}^2 - g_\mathrm{h}(F_z))]\right]. \tag{14}$$

Although this expression is similar in structure to the phenomenological formula used by Oesterhelt *et al* [6] it is considerably more detailed as more microscopic information is contained in it.

Finally, we give the entropy as a function of temperature and extension

$$s(T,L) = -\left.\frac{\partial f(T,L)}{\partial T}\right|_L = -k_\mathrm{B}\frac{f(T,L)}{k_\mathrm{B}T} + k_\mathrm{B}\Big(\sum_{i'} Z_{i'}\Big)^{-1}\sum_i Z_i\Big(\frac{V_i}{k_\mathrm{B}T} + T\frac{\partial}{\partial T}\sum_k \ln z_k^{(i)}\Big). \tag{15}$$

3. Results

We have evaluated the force–extension relation for $(\mathrm{EG})_3$ in vacuum and also solvated in water, both under isothermal–isochoric and under isothermal–isobaric conditions.

We begin with $(\mathrm{EG})_3$ in vacuum and base the calculations in equation (7) on the potential energy curves of figure 2. Under isothermal–isobaric conditions, as implemented in the experiment, the force–extension curve at 300 K is shown as a full curve in figure 4. Starting at the shortest extension the force is negative as one descends into the energy minimum of the buckled ($g^+g^+g^-$) conformer. One then needs a positive force to stretch this conformer to the point where the helical ($g^+g^+g^+$) conformer is energetically more favourable. This low-force response continues as long as further conformers with larger extension are energetically within $k_\mathrm{B}T$, for our system this is the case for the (g^+tt) conformer. Once the transformation to the planar (ttt) conformer has happened we leave the low-force regime, characteristic of transformations between different conformers. Much larger forces, given by the slope of the narrow (ttt) potential energy curve, are required to further stretch the bonding angles in the 'all-trans' conformer.

Only the positive part of the force–extension curve is relevant for comparison with experiment for two reasons: (i) only stretching forces are applied in the experiment, and (ii)

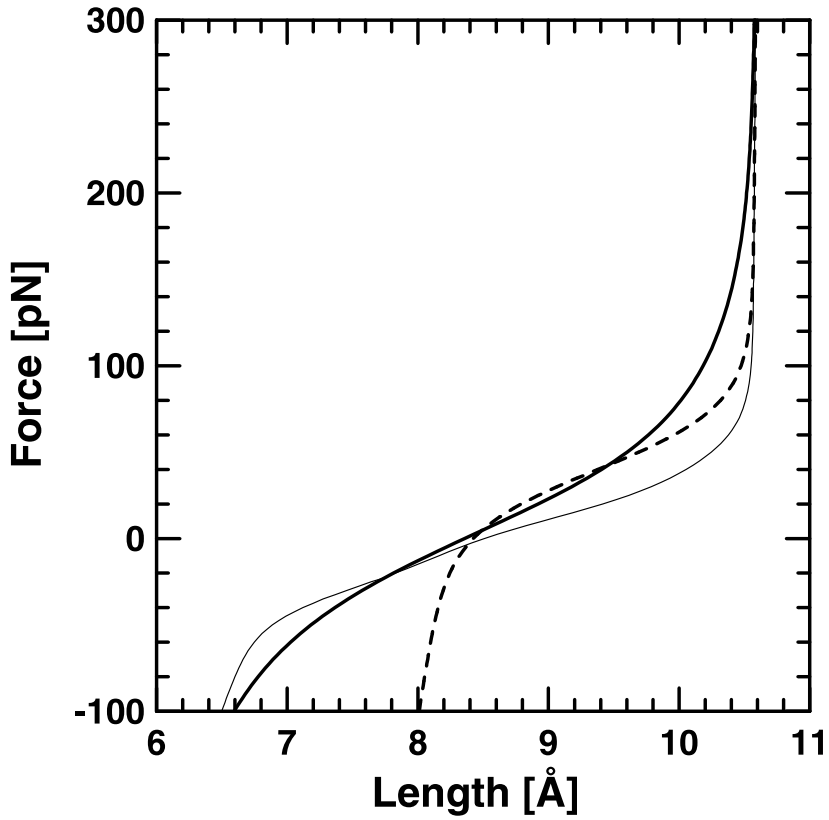

Figure 4. Force–extension curves under isothermal–isobaric conditions for $(\mathrm{EG})_3$ in vacuum, calculated from (7) based on the potential energy curves of figure 2. Thick curve at 300 K, thin curve at 100 K, dotted curve at 300K, but with only the helical and 'all-trans' conformers.

a long polymer strand (of 750 EG units as used in the experiment) would avoid a compressive force by large-scale buckling or folding. This is not possible for our short $(\mathrm{EG})_3$ strands. Indeed, if we eliminate the (buckled) $g^+g^+g^-$ energy curve from the calculations the force drops to negative values much faster as one climbs the short-distance wall of the $g^+g^+g^+$ curve. This effect is demonstrated by the broken curve in figure 4 for which we have also eliminated the ttg^+ curve to make contact with the two-state model of Oesterhelt *et al* [6]. It is clear that the low-force regime is extended over a larger range of lengths if more conformers (potential energy curves) with minima within $k_\mathrm{B}T$ participate. The number of such conformers (only four or five for $(\mathrm{EG})_3$) increases rapidly with the length of the $(\mathrm{EG})_n$ molecule. As for temperature effects the thin curve in figure 4 shows the response at 100 K; it is flatter and more abrupt as one would expect. In particular, the stepwise increase in the force at a length of 8.3 Å is indicative of the transition from the $g^+g^+g^+$ to the g^+tt conformer.

As we discussed above, the experiment is performed under isothermal–isobaric conditions as were the calculations shown in figure 4. To shed more light on the problem we next show the response under isothermal–isochoric conditions, using the expression (5), in figure 5. Clearly, by fixing the length of the molecule both negative and positive forces will be measured as the extension is increased, the changes from positive to negative forces occurring as one crosses the

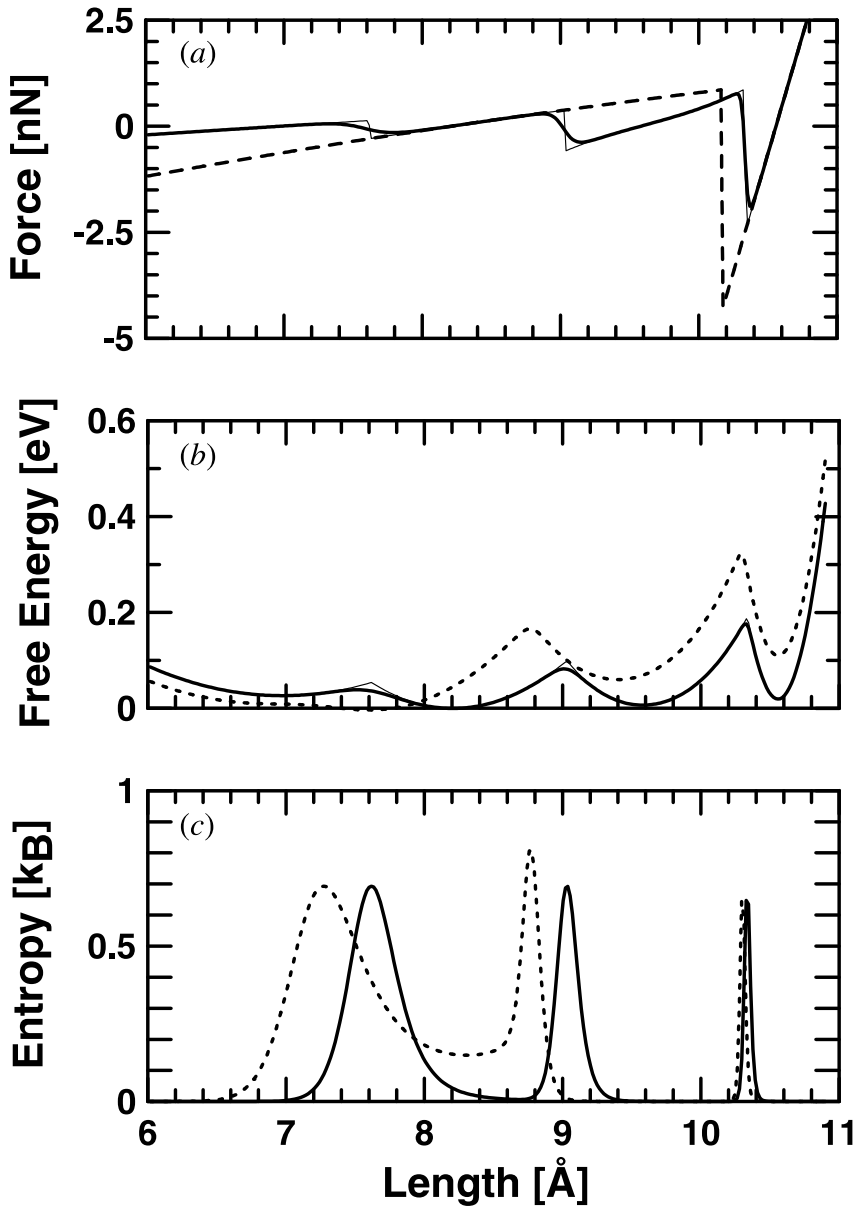

Figure 5. Isothermal–isochoric conditions: (*a*) force–extension curves for the potential energy curves of figure 2: thick curve at 300 K, thin curve at 10 K and dotted curve with only the helical and 'all-trans' conformers. (*b*) Helmholtz free energy in vacuum (thick curve at $T = 300$ K and thin curve at $T = 1$ K) and solvated (broken curve). (*c*) Entropy in vacuum (thick curve) and solvated (broken curve) at $T = 300$ K.

intersection of two of the energy curves (given in figure 2). The changeover from an attractive to a repulsive force is discontinuous at zero temperature, where it is simply the derivative of the lowest (at a given extension) potential curve; this is shown as the thin curve in figure 5. We also show the situation where we (artificially) eliminate all but the $g^+g^+g^+$ and ttt potential energy curves in which case only one crossover occurs (broken curve). This case is suited to extracting

the isothermal stretching modulus for the two conformers,

$$K_{\mathrm{s}} = N_{\mathrm{s}} \frac{\partial F}{\partial L}\bigg|_{T}. \tag{16}$$

For the helical and 'all-trans' conformers we find 5 and 102 N m^{-1}, respectively, in agreement with the force constants given in the text below table 1. Although the latter (theoretical) value is only two thirds of what the fit of the experimental data to the phenomenological model produces (150 N m^{-1}) this is not in contradiction with experiment. Indeed, the interpretation of the parameters of the freely joined chain model is rather tenuous, if not completely impossible†.

In figure 5 we also show in the centre panel the Helmholtz free energy and, in the lower panel, the entropy as a function of length for fixed temperature. The temperature dependence is rather weak up to room temperature implying (i) that the internal energy is quite close to the $T = 0$ K Helmholtz free energy. These curves more or less trace the potential energy curves of figure 2 with the crossovers between two conformers rounded. In the lower panel of figure 5 we show the entropy which, not surprisingly, is only substantially different from zero at room temperature at the crossover points, i.e. at the maxima of the free-energy curve, because only there is there some disorder associated with the choice of the system being in either one of the two crossing conformers. Extending the calculations to high temperatures (so much higher than room temperature that the maxima in the (low-temperature) free energy can be easily overcome) we find that the (room-temperature) maxima in the free energy and the entropy wash out, and the entropy eventually reaches a value of $k_{\mathrm{B}} \ln 4$ because, for a fixed length, our model is one involving four states. We note that any configurational entropy (e.g. as modelled by the freely jointed chain model) has been reduced to zero at the late stages of stretching the polymer.

To understand the important factors that control the shape of the force–extension relation under isobaric conditions we have performed a series of model calculations varying the number, relative energies and widths of the potential energy curves. For two potential energy curves with minima within $k_{\mathrm{B}}T$ we find a low-force regime over the distance between the minima of the two potential energy curves (see figures 6(*a*) and (*b*)). The high-force regime at larger extensions is then controlled by the steepness of the longer conformer. The effect of the width of the lower energy curve is then minimal; likewise, one can lower the minimum of the potential energy curve of the longer conformer without significant changes. A third potential energy curve, again with a minimum within $k_{\mathrm{B}}T$ of the other two does not alter the picture (figures 6(*c*) and (*d*)), neither does a series of potential energy curves with monotonically rising minima, (figures 6(*e*) and (*f*)). Lastly, if in a series of overlapping curves, such as the three in figure 6(*g*), the minima of the curves first decrease, followed by a last potential with a considerably higher minimum, then the low-force plateau is followed by a short rise of intermediate slope followed by the familiar high-force regime (see figure 6(*h*)). This is very much akin to what is seen experimentally when the EG moities are dissolved in water.

We have calculated the force–extension relation for solvated $(\mathrm{EG})_3$ based on the potential energy curves in figure 3 and get the broken curve in figure 7, where, for comparison with the experiment, we only show the response for positive forces (pull). Also note that for a

† This point is discussed at length by Flory in the introduction to his book where among other things he says 'Thus no matter how faithfully such a model (the freely jointed chain) may represent experimental observations, interpretations carried out in its terms are cast in a framework of unreality. The properties deduced for the hypothetical segment defy transcription to the real chain.'

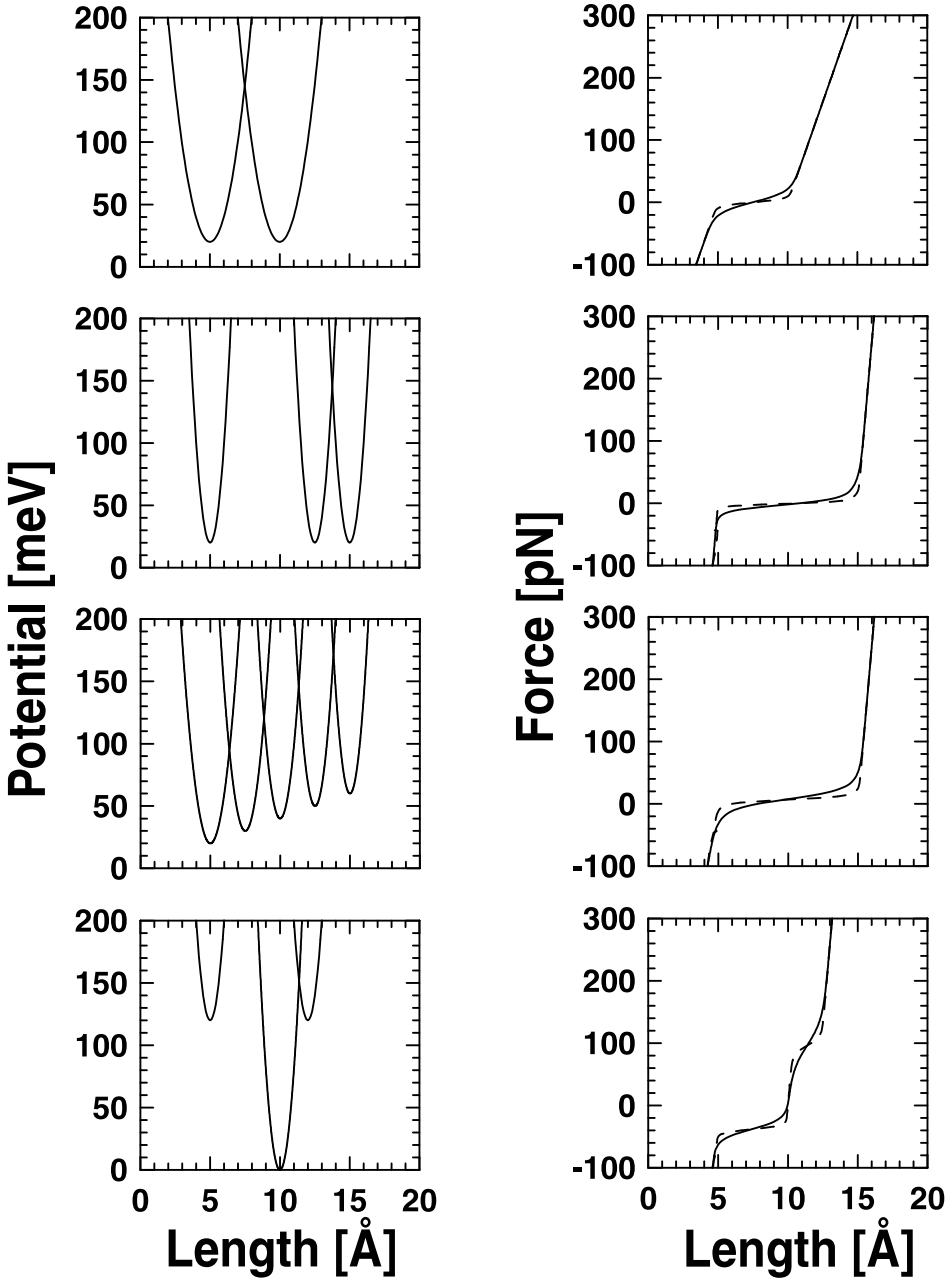

Figure 6. Model potential energy curves and resulting force–extension curves.

direct comparison with the data by Oesterhelt *et al*, one must divide the length axis by 3 to get the length per EG unit†. Clearly the qualitative difference in the force–extension curves for PEG in hexadecane and in PBS are reproduced by our theory and can be traced to the energetic differences in the attachment of water to the 'all-trans' conformer as opposed to the

† In a detailed comparison with the data of Oesterhelt *et al* we found a discrepancy in the length scale. It turned out that the scale of figure 5 of Oesterhelt *et al* is not quite right and should be reduced by a factor 0.94 (P Oesterhelt, private communication) which then gives excellent agreement between theory and experiment. This comparison, together with an extension of the present work, will be reported elsewhere.

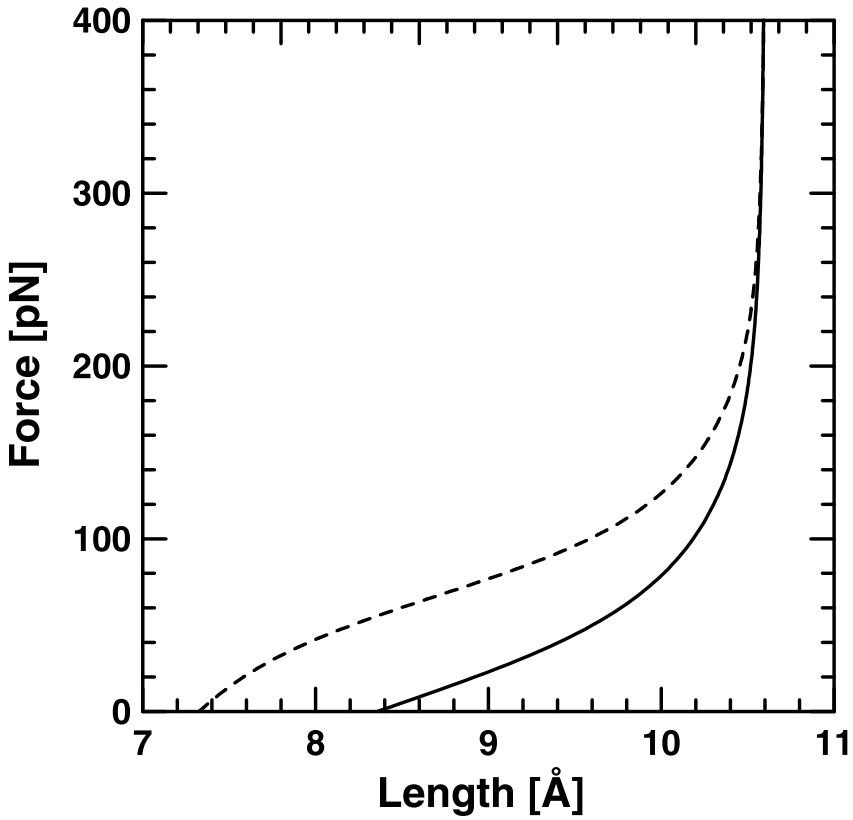

Figure 7. Force–extension curves for pure (full curve) and solvated (broken curve) $(\mathrm{EG})_3$. The length scale must be divided by 3 to get the length per EG unit for a direct comparison with the data of figure 5 by Oesterhelt *et al*. (The length scale in figure 5 of Oesterhelt *et al* must be reduced by a factor 0.94, see the previous footnote.)

other conformers containing at least one gauche segment.

We repeat a statement made above in connection with the model calculations of figure 6, namely that the width of the shorter conformers does not affect the shape of the force–extension curve significantly, for instance, halving the width of the potential energy curve of the shortest conformer only shifts the onset of the positive part of the force–extension curve by 0.1 Å.

To shed more light on the physics of solvation we have also calculated the Helmholtz free energy and the entropy, shown as dotted curves in the central and lower panels of figure 5, respectively. As expected the peaks in both functions are shifted with the respect to those of $(\mathrm{EG})_3$ in vacuum and the effect of solvation is largest in the intermediate-force regime before the transition to the 'all-trans' conformer occurs.

Our calculations also confirm that the low- and high-force regimes can be satisfactorily modelled by a two-state model including the helical and 'all-trans' conformers as the most extreme. However, to understand the intermediate-force regime of the hydrated moities at least three conformers should be included. This point also strongly suggests that the theory should be extended to longer molecules, such as $(\mathrm{EG})_7$, which automatically will have more, energetically close, conformers.

To compare our results in more detail to the phenomenological two-state model of Oesterhelt *et al* we note that our *ab initio* calculations give an energy difference between the helical and planar conformers of 19.2 meV increasing to 110 meV when water is present. The trend is, at least qualitatively, close to what they find, i.e. energy differences of $k_{\mathrm{B}}T$ and $3k_{\mathrm{B}}T$, respectively, at $T = 300$ K.

Acknowledgments

We acknowledge financial support of this work by the Office of Naval Research, Deutsche Forschungsgemeinschaft, and Verband der Chemischen Industrie.

References

[1] Lee G U, Kidwell D A and Colton R J 1994 *Langmuir* **10** 354
[2] Moy V T, Florin E L and Gaub H E 1994 *Science* **266** 257
[3] Rief M, Gautel M, Oesterhelt F, Fernandez J M and Gaub H E 1997 *Science* **276** 1109
[4] Rief M, Oesterhelt F, Heymann B and Gaub H E 1997 *Science* **275** 1295
[5] Wang R L, Kreuzer H J and Grunze M *J. Phys. Chem.* 1997 B **101** 9767
[6] Oesterhelt F, Rief M and Gaub H E 1999 *New J. Phys.* **1** 6
[7] Lüsse S and Arnold K 1996 *Macromolecules* **29** 4251
[8] Zolk M, Buck M, Eisert F, Grunze M, Wang R L C and Kreuzer H J, in preparation
[9] Flory P J 1969 *Statistical Mechanics of Chain Molecules* (New York: Interscience)